

Shot noise as a diagnostic in the $\nu = 2/3$ fractional quantum Hall edge zoo

Sourav Manna,^{1,2,*} Ankur Das,^{1,3,†} Yuval Gefen,¹ and Moshe Goldstein²

¹*Department of Condensed Matter Physics, Weizmann Institute of Science, Rehovot 7610001, Israel*

²*Raymond and Beverly Sackler School of Physics and Astronomy, Tel-Aviv University, Tel Aviv, 6997801, Israel*

³*Department of Physics, Indian Institute of Science Education and Research (IISER) Tirupati, Tirupati 517619, India*

The $\nu = 2/3$ filling is the simplest paradigmatic example of a fractional quantum Hall state, which contains counter-propagating edge modes. These modes can be either in the unequilibrated regime or equilibrated to different extents, on top of a possible edge reconstruction. In the unequilibrated regime, two distinct renormalization group fixed points have been previously proposed, namely Kane-Fischer-Polchinski and Wang-Meir-Gefen. In the equilibration regime, different degree of thermal equilibration may occur, while charge is fully equilibrated. Here, we show that this rich variety of models can give rise to three possible conductance plateaus at $e^2/2h$ (recently observed in experiments), $5e^2/9h$ (predicted here), and $e^2/3h$ (observed earlier in experiments) in a quantum point contact geometry. We identify different mechanisms for *electrical shot noise* generation at these plateaus, which provides an experimentally accessible venue for distinguishing among the distinct models.

The tragic and barbaric killing of Prof. Sergei Gre-deskul and his wife, Viktoria, as they spent a quiet week-end at home on the accursed October 7th, 2023, was one of many tragedies that happened on that day and the following months. A student of Ilya Lifshitz, and a scientific grandson of Lev Landau, Sergei left a great career at Kharkiv University, Ukraine, and moved in 1991 to Israel, where he became a member of the Physics Department at Ben Gurion University. Sergei made numerous contributions to condensed matter physics; a common theme that can be found in many of his works is disorder and inhomogeneity. Even those who did not know him closely felt that Sergei deserved a scientific commemoration, and we are proud to be part of this endeavor.

I. INTRODUCTION

The fractional quantum Hall (FQH) effect [1, 2] serves as an important platform for studying topologically ordered phases of matter. This remarkable phenomenon manifests itself in a gapped bulk with gapless chiral edges, realizing the bulk-boundary correspondence. The edge modes can carry both charge and energy. They may either be co-propagating or counter-propagating. Interaction and disorder may give rise to emergent edge renormalization (for the case of counter-propagating modes), with the $\nu = 2/3$ state serving as the simplest example [3, 4]. The early proposal by MacDonald postulated the edge modes to be e and $e/3$ charge modes [3, 5, 6]. However, this proposed edge structure failed to provide a picture consistent with the experimental observations, namely two-terminal electrical conductance of $2e^2/3h$, and the failure to detect a counter-propagating $e/3$ charge mode [7].

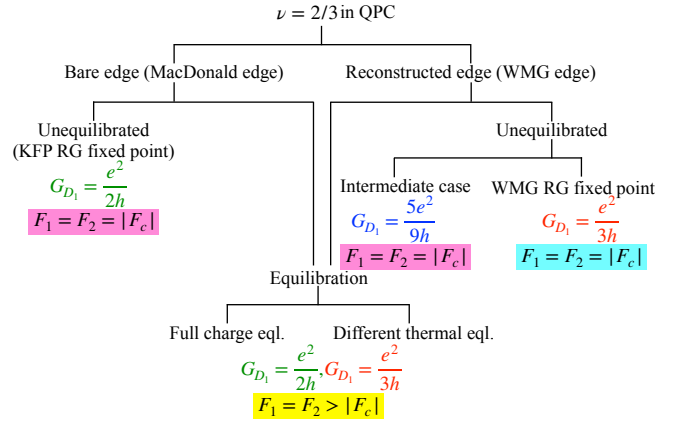


FIG. 1. Color-coded conductance plateaus (G_{D_1}) and shot noise Fano factor (F_1, F_2, F_c) inequalities: $e^2/2h$ QPC plateau (green) arises from either unequilibrated or equilibrated regimes, which are distinguishable by distinct Fano factor inequalities (pink and yellow), and similarly for the $e^2/3h$ QPC plateau. The $5e^2/9h$ QPC plateau originates only in the unequilibrated regime.

Eventually, it was proposed that random disorder induced charge tunneling between the counter-propagating modes may play a crucial role [4]. It was shown that, at zero temperature, the system approaches a disorder dominated coherent renormalization group (RG) fixed point, known as the Kane-Fischer-Polchinski (KFP) RG fixed point [4]. At this fixed point the edge consists of a $2e/3$ charge mode counter-propagating to a neutral mode. This edge structure is consistent with the experimentally observed two-terminal electrical conductance of $2e^2/3h$.

A somewhat more complicated experimental device which can provide more information regarding the edge structure is a quantum point contact (QPC), a constriction in the two-dimensional electron gas [8]. Across the QPC, shot noise can be measured to determine the charge carried by an edge mode [9–15]. For $\nu = 2/3$, the ob-

* sourav.manna@weizmann.ac.il

† ankur@labs.iisertirupati.ac.in

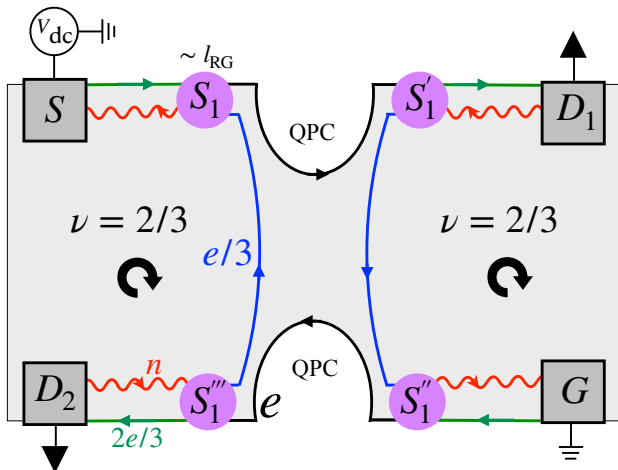


FIG. 2. $1/2$ QPC conductance plateau in the stochastic case: A Hall bar with bulk filling $\nu = 2/3$ in a QPC. The device contains a source S (with dc voltage V_{dc}), a ground contact G , and two drains, D_1 and D_2 . From the contacts emanate renormalized modes. The charge propagation chirality is depicted by a circular arrow. The scattering regions (purple circles) with size l_{RG} are defined by the density kernel matrices S_1, S'_1, S''_1, S'''_1 [25]. Here S'_1 and S''_1 account for the stochastic processes and S_1 and S'''_1 give rise to deterministic charge propagation.

servation of a $e^2/3h$ QPC conductance plateau [16, 17], measurements consistent with the existence of neutral modes [18], and a crossover of the effective charge while changing the temperature [17] were found. These are incompatible with the KFP RG fixed point. To accommodate these experimental findings, reconstruction of the MacDonald edge was proposed leading to a new coherent intermediate RG fixed point, proposed by Wang-Meir-Gefen (WMG) [19]. At this fixed point the edge consists of two $e/3$ charge modes counter-propagating to two neutral modes.

The existence of a plateau at a fractional QPC transmission (corresponding to a QPC filling) and shot noise therein can also be a consequence of equilibration among the chiral edge modes [20] at finite temperatures. Charge and heat equilibrations can occur independently. Recently, different experiments [21–24] have confirmed that the thermal equilibration length is order of magnitude larger than the charge equilibration length. These findings have complicated the study of the steady state of edges since different regimes of thermal equilibration can occur while charge is fully equilibrated.

In this paper we show in details ([26] contains the non-technical insight) that these zoo of models can give rise to three distinct QPC conductance plateaus at $e^2/2h$, $5e^2/9h$, and $e^2/3h$. We note that the $e^2/2h$ plateau has been reported recently [27, 28] and the $e^2/3h$ plateau was discovered earlier [17] in experiments. We predict the possible appearance of $5e^2/9h$ plateau. We identify different scenarios for each plateau, as well as different mechanisms which may give rise to *electrical shot noise* at these plateaus. We show how shot noise can

be used to experimentally discern between the different models (we refer to Fig. 1 for a flowchart, summarizing our findings). The rest of this paper is structured as follows: We explain the emergence of $e^2/2h$, $5e^2/9h$, and $e^2/3h$ QPC conductance plateaus and calculate the shot noise for each in Section II, Section III, and Section IV, respectively. We provide a summary and an outlook in Section V.

II. THE NOISY $e^2/2h$ QPC PLATEAU

The recently observed $e^2/2h$ QPC conductance plateau [27, 28] is analyzed in this section (see also Refs. 29–31). We derive different inequalities among autocorrelations and crosscorrelation in the unequilibrated and equilibrated regimes.

A. Unequilibrated scenario

We briefly mention that in the fully coherent case, two distinct scenarios may occur: either no QPC conductance plateau, or a noiseless QPC plateau at the same conductance as we find below [26]. We therefore assume that the wavepackets undergo incoherent scattering in each region of size l_{RG} (Fig. 2). Density kernel matrices S_1, S'_1, S''_1, S'''_1 [25] quantify such processes. We note that S'_1 and S''_1 give rise to the stochastic processes, while S_1 and S'''_1 give rise to deterministic processes. Hence, we write

$$\begin{aligned} S_1 &= \begin{pmatrix} T_{11} & R_{21} \\ R_{12} & T_{22} \end{pmatrix} = S'''_1, \\ S'_1 &= \begin{pmatrix} \langle T'_{11} \rangle & \langle R'_{21} \rangle \\ \langle R'_{12} \rangle & \langle T'_{22} \rangle \end{pmatrix} = S''_1, \end{aligned} \quad (1)$$

where T', T''', R', R''' are Bernoulli random numbers $\in \{0, 1\}$, while T, T'', R, R'' are deterministic. The average value over the stochastic variable distribution] is denoted by $\langle \dots \rangle$.

The total charge, reaching each drain, is determined by summing up an infinite series arising from multiple reflections and transmissions. This series contains the following pieces:

1. First tunnelling factor to enter the QPC.
2. Shortest path inside the QPC.
3. Contribution due to multiple reflections from different scatterers: $(R'_{12})_i (R''_{21})_i (R'''_{12})_i (R_{21})_{i+1}$, $i \in [1, 2, \dots]$, which is the same for all the contacts.

For the charge Q_1 which enters the drain D_1 the first piece is $(T_{11})_1$, and the second piece is $(T'_{11})_n$, $n \in [1, 2, \dots]$. How many times a wavepacket encountered the same scatterer is denoted by the subscript outside of the parenthesis. Therefore, we write Q_1 as

$$\begin{aligned}
Q_1 = \frac{2e}{3} & \left[(T_{11})_1 (T'_{11})_1 + (T_{11})_1 (R'_{12})_1 (R''_{21})_1 (R'''_{12})_1 (R_{21})_2 (T'_{11})_2 \right. \\
& + (T_{11})_1 (R'_{12})_1 (R''_{21})_1 (R'''_{12})_1 (R_{21})_2 (R'_{12})_2 (R''_{21})_2 (R'''_{12})_2 (R_{21})_3 (T'_{11})_3 \\
& \left. + (T_{11})_1 (R'_{12})_1 (R''_{21})_1 (R'''_{12})_1 (R_{21})_2 (R'_{12})_2 (R''_{21})_2 (R'''_{12})_2 (R_{21})_3 (R'_{12})_3 (R''_{21})_3 (R'''_{12})_3 (R_{21})_4 (T'_{11})_4 + \dots \right].
\end{aligned} \tag{2}$$

We point out the following conditions (and similarly for T''' , R'''),

$$\begin{aligned}
(T'_{11})_i + (R'_{12})_i &= 1, \quad (T'_{11})_i (R'_{12})_i = 0, \\
(T'_{22})_i + (R'_{21})_i &= 1, \quad (T'_{22})_i (R'_{21})_i = 0,
\end{aligned} \tag{3}$$

and any T' and R' are uncorrelated for distinct scattering event indices i . We further assume that transmission and reflection coefficients having different inner indices become uncorrelated since they correspond to different scatterers. Thus,

$$\langle Q_1 \rangle = \frac{2e}{3} \left[\frac{T_{11} \langle T'_{11} \rangle}{1 - \langle R'_{12} \rangle R''_{21} \langle R'''_{12} \rangle R_{21}} \right]. \tag{4}$$

Using $T_{11} = 1$, $\langle T'_{11} \rangle = 2/3$, $\langle R'_{12} \rangle = \langle R''_{12} \rangle = 1/3$, $R''_{21} = R_{21} = 1$, we find $\langle Q_1 \rangle = e/2$. The source current is $I = 2e/3\tau$ and the transmission coefficient becomes $t = \langle Q_1 \rangle / \tau I = 3/4$ and the QPC conductance plateau is at $G_{D_1} = 1/2$. The charge reaching D_2 is $\langle Q_2 \rangle = 2e/3 - \langle Q_1 \rangle = e/6$.

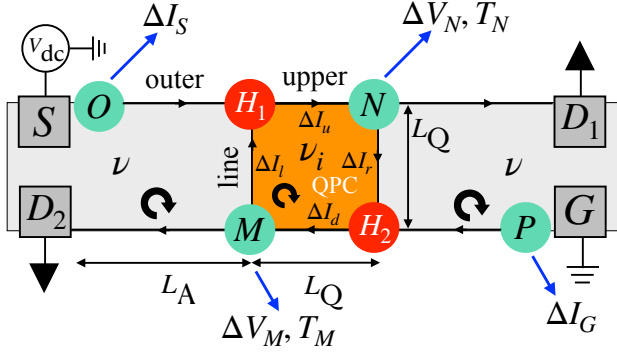


FIG. 3. $1/2$ QPC conductance plateau in the equilibrated case: The set up is similar to Fig. 2. The bulk filling is $\nu (= 2/3)$ and the QPC filling is $\nu_i (= 1)$. We have the geometric lengths: L_A , L_Q . We denote the segment between the vacuum and ν as “outer”, between the vacuum and ν_i as “upper”, and between ν and ν_i as “line”. In each segment, the arrow shows the fully equilibrated charge propagation. Hot spots H_1 , H_2 (red circles) are created due to the voltage drops there, leading in turn to the formation of noise spots M , N , O , P (green circles) [20].

For the autocorrelation $\delta^2 Q_1 = \langle Q_1^2 \rangle - \langle Q_1 \rangle^2 = \langle Q_1 \rangle (2e/3 - \langle Q_1 \rangle)$, since $\langle Q_1^2 \rangle = 2e \langle Q_1 \rangle / 3$, at D_1 we obtain $\delta^2 Q_1 = e^2/12$. Similarly, we write for the autocorrelation $\delta^2 Q_2 = \langle Q_2^2 \rangle - \langle Q_2 \rangle^2$ at D_2 we obtain $\delta^2 Q_2 = e^2/12$ and the crosscorrelation $\delta^2 Q_c = \langle Q_1 Q_2 \rangle - \langle Q_1 \rangle \langle Q_2 \rangle = -\langle Q_1 \rangle \langle Q_2 \rangle$ (since $\langle Q_1 Q_2 \rangle = 0$) becomes $\delta^2 Q_c = -e^2/12$.

The Fano factors are defined as

$$F_i = \frac{\delta^2 Q_i}{e \tau I t (1 - t)}, \quad i \in \{1, 2, c\}, \tag{5}$$

and therefore they evaluate to be $F_1 = F_2 = -F_c = 2/3$.

B. Equilibrated scenario

For bulk filling ν and QPC filling ν_i with $\nu < \nu_i$ (Fig. 3), we derive analytical expressions for the current-current correlations (CCC) (shot noise). We assume a fully equilibrated charge transport, which is ballistic, moving “downstream” along a segment. We take no bulk-leakage [32–35] and assume that the lead contacts are at zero temperature.

We consider Fig. 3 and follow Refs. [20, 36] to write

$$\begin{aligned}
\Delta I_S + \Delta I_l &= \Delta I_u, \\
\Delta I_u &= \Delta I_1 + \Delta I_r, \\
\Delta I_G + \Delta I_r &= \Delta I_d, \\
\Delta I_d &= \Delta I_2 + \Delta I_l,
\end{aligned} \tag{6}$$

where ΔI_i , $i \in \{S, G, u, d, r, l, 1, 2\}$ are the current fluctuations. We also write

$$\begin{aligned}
\Delta I_1 &= \nu \frac{e^2}{h} \Delta V_N + \Delta I_1^{\text{th}}, \\
\Delta I_r &= (\nu_i - \nu) \frac{e^2}{h} \Delta V_N + \Delta I_r^{\text{th}}, \\
\Delta I_2 &= \nu \frac{e^2}{h} \Delta V_M + \Delta I_2^{\text{th}}, \\
\Delta I_l &= (\nu_i - \nu) \frac{e^2}{h} \Delta V_M + \Delta I_l^{\text{th}},
\end{aligned} \tag{7}$$

where ΔV_i , $i \in \{M, N\}$ are the voltage fluctuations and ΔI_i^{th} , $i \in \{1, 2, r, l\}$ are the thermal fluctuations. We find

$$\begin{aligned}
\Delta I_1 &= \frac{1}{(\nu - 2\nu_i)} \left[(\nu - \nu_i) (\Delta I_G + \Delta I_1^{\text{th}} - \Delta I_2^{\text{th}}) \right. \\
& \quad \left. - \nu (\Delta I_l^{\text{th}} - \Delta I_r^{\text{th}}) - \nu_i \Delta I_S \right], \\
\Delta I_2 &= \frac{1}{(\nu - 2\nu_i)} \left[(\nu - \nu_i) (\Delta I_S - \Delta I_1^{\text{th}} + \Delta I_2^{\text{th}}) \right. \\
& \quad \left. + \nu (\Delta I_l^{\text{th}} - \Delta I_r^{\text{th}}) - \nu_i \Delta I_G \right].
\end{aligned} \tag{8}$$

We use the local Johnson-Nyquist relations for thermal

noise,

$$\begin{aligned}
\langle(\Delta I_l^{\text{th}})^2\rangle &= \frac{2e^2}{h}(\nu_i - \nu)k_B T_M, \\
\langle(\Delta I_1^{\text{th}})^2\rangle &= \frac{2e^2}{h}\nu k_B T_N, \\
\langle(\Delta I_r^{\text{th}})^2\rangle &= \frac{2e^2}{h}(\nu_i - \nu)k_B T_N, \\
\langle(\Delta I_2^{\text{th}})^2\rangle &= \frac{2e^2}{h}\nu k_B T_M, \\
\langle(\Delta I_i^{\text{th}}\Delta I_j^{\text{th}})\rangle &= 0, \text{ for } i \neq j \text{ and } i, j \in \{1, 2, l, r\},
\end{aligned} \tag{9}$$

where k_B is the Boltzmann constant to write

$$\begin{aligned}
\delta^2 I_1 &= 2 \left(\frac{e^2}{h} \right) \frac{\nu\nu_i(\nu_i - \nu)}{(\nu - 2\nu_i)^2} k_B (T_M + T_N) \\
&+ \frac{1}{(\nu - 2\nu_i)^2} \left[\nu_i^2 \langle(\Delta I_S)^2\rangle + (\nu - \nu_i)^2 \langle(\Delta I_G)^2\rangle \right],
\end{aligned} \tag{10}$$

$$\begin{aligned}
\delta^2 I_2 &= 2 \left(\frac{e^2}{h} \right) \frac{\nu\nu_i(\nu_i - \nu)}{(\nu - 2\nu_i)^2} k_B (T_M + T_N) \\
&+ \frac{1}{(\nu - 2\nu_i)^2} \left[\nu_i^2 \langle(\Delta I_G)^2\rangle + (\nu - \nu_i)^2 \langle(\Delta I_S)^2\rangle \right],
\end{aligned} \tag{11}$$

and

$$\begin{aligned}
\delta^2 I_c &= -2 \left(\frac{e^2}{h} \right) \frac{\nu\nu_i(\nu_i - \nu)}{(\nu - 2\nu_i)^2} k_B (T_M + T_N) \\
&+ \frac{\nu_i(\nu_i - \nu)}{(\nu - 2\nu_i)^2} \left[\langle(\Delta I_S)^2\rangle + \langle(\Delta I_G)^2\rangle \right],
\end{aligned} \tag{12}$$

where the noise spot (M and N) temperatures are T_M, T_N , respectively [20, 36]. The dissipated powers at the hot spots is

$$P_{H_1} = P_{H_2} = \frac{e^2 V_{\text{dc}}^2}{h} \frac{\nu(\nu_i - \nu)}{2\nu_i} \left(\frac{\nu_i}{2\nu_i - \nu} \right)^2. \tag{13}$$

The contributions $\langle(\Delta I_G)^2\rangle = \langle(\Delta I_S)^2\rangle$ at the noise spots O and P can be calculated in a similar way as shown in Ref. 20 and 36. The Joule heating term provides a negligible contribution to the noise spots [20, 36].

We consider $\{\nu, \nu_i\} = \{2/3, 1\}, \{2/3(r), 1\}$, and $\{2/3(r), 1(r)\}$, where $2/3(r)$ denotes the reconstructed MacDonald edge [19, 37] having filling factor discontinuity $\delta\nu = [-1/3, +1, -1/3, +1/3]$ (Fig. 3). Also $1(r)$ refers to the edge reconstruction in QPC, with the discontinuity $\delta\nu_i = [+1, -1/3, +1/3]$ (Fig. 3) [38]. For full charge equilibration (Fig. 3), we have

$$I_1 = \frac{e^2 V_{\text{dc}}}{h} \times \frac{2}{3} \times \frac{2}{3} \times \sum_{i=0}^{\infty} \left(\frac{1}{3^2} \right)^i = \frac{e^2 V_{\text{dc}}}{2h} \tag{14}$$

for each of the $\{\nu, \nu_i\}$ choices, which leads to the transmission $t = 3/4$ and $G_{D_1} = 1/2$.

Three distinct thermal equilibration regimes are considered (taking $l_{\text{eq}}^{\text{th}}$ as the thermal equilibration length): (i) each segment of the device is thermally unequilibrated leading to $L_Q \ll L_A \ll l_{\text{eq}}^{\text{th}}$ (no thermal equilibration); (ii) only the QPC segment is thermally unequilibrated while all other segments are thermally equilibrated leading to $L_Q \ll l_{\text{eq}}^{\text{th}} \ll L_A$ (hybrid thermal equilibration); (iii) or each segment is thermally equilibrated leading to $l_{\text{eq}}^{\text{th}} \ll L_Q \ll L_A$ (full thermal equilibration). Ref. 23 also studied the thermally unequilibrated case for a single edge. We note that only the upstream modes from $H_1(H_2)$ contribute to $O(P)$ in the no thermal equilibration regime, as the downstream modes become fully thermally isolated from the upstream modes and have zero temperature.

Below we compute the CCC values for $\{\nu, \nu_i\} = \{2/3, 1\}$ in the no thermal equilibration regime. Energy conservation at H_1, M leads to [20, 36] :

$$\begin{aligned}
J_S + J_l + P_{H_1} &= J_u, \\
J_d &= J_l + J_2,
\end{aligned} \tag{15}$$

where the heat current J_i flows along the segment $i \in \{S, l, u, d, 2\}$. We write

$$\begin{aligned}
J_S &= -\frac{\kappa}{2} T_{H_1}^2, J_l = \frac{\kappa}{2} (2T_M^2 - T_{H_1}^2), \\
J_u &= \frac{\kappa}{2} T_{H_1}^2, J_d = \frac{\kappa}{2} T_{H_2}^2, J_2 = \frac{\kappa}{2} T_M^2,
\end{aligned} \tag{16}$$

where $\kappa = \frac{\pi^2 k_B^2}{3h}$ and $T_{H_1} = T_{H_2}$ and $T_M = T_N$ are the temperatures at H_1, H_2, M, N , respectively. We find

$$T_M = T_N = \frac{3\sqrt{4}eV_{\text{dc}}}{4\sqrt{15}\pi k_B}, T_{H_1} = T_{H_2} = \frac{3\sqrt{2}eV_{\text{dc}}}{4\sqrt{5}\pi k_B}. \tag{17}$$

The contribution from the noise spots O and P is evaluated to [20, 36]

$$\langle(\Delta I_S)^2\rangle = \langle(\Delta I_G)^2\rangle \approx 0.0472 \frac{e^3 V_{\text{dc}}}{h} \tag{18}$$

leading to $F_1 = F_2 \approx 0.36, F_c \approx -0.17$.

In a similar manner, for $\{\nu, \nu_i\} = \{2/3(r), 1\}$ we find

$$\begin{aligned}
T_M = T_N &= \frac{3eV_{\text{dc}}}{16\pi k_B}, \\
\langle(\Delta I_S)^2\rangle &= \langle(\Delta I_G)^2\rangle \approx 0.048 \frac{e^3 V_{\text{dc}}}{h},
\end{aligned} \tag{19}$$

leading to $F_1 = F_2 \approx 0.23, F_c \approx -0.04$. For $\{\nu, \nu_i\} = \{2/3(r), 1(r)\}$ we find

$$\begin{aligned}
T_M = T_N &= \frac{3\sqrt{5}eV_{\text{dc}}}{4\sqrt{36}\pi k_B}, \\
\langle(\Delta I_S)^2\rangle &= \langle(\Delta I_G)^2\rangle \approx 0.065 \frac{e^3 V_{\text{dc}}}{h},
\end{aligned} \tag{20}$$

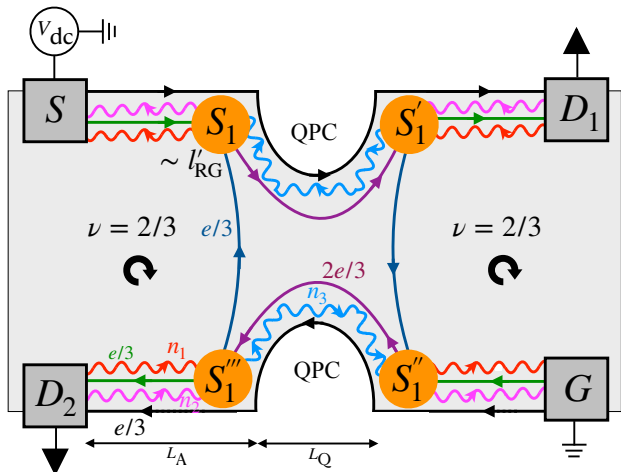


FIG. 4. The stochastic scenario for the $5/9$ QPC conductance plateau where the normalized modes emanate from the contacts. The set up is similar to Fig. 2. The reconstructed MacDonald edge structure consists of counter-propagating $e/3$ (innermost), $e, e/3$ and $e/3$ (outermost) charge modes (from bulk to edge) [19]. At the QPC one $e/3$ mode (outermost) transmits fully and the other $e/3$ mode (innermost) backscatters fully. The rest of the modes are renormalized to a $2e/3$ charge mode and n_3 neutral mode (counter-propagating) at the KFP RG fixed point [4] (KFP region). Between a contact and QPC we have n_1, n_2 neutral modes and two $e/3$ charge modes (counter-propagating) [19] (WMG region). Near QPC, we have regions of size l'_{RG} (orange circles). We define these regions by using density kernel matrices S_1, S_1', S_1'', S_1''' [25] constructed out of the transmission and reflection coefficients. We note that S_1' and S_1''' describe stochastic processes while S_1 and S_1'' describe deterministic ones.

leading to $F_1 = F_2 \approx 0.33$ and $F_c \approx -0.07$. In a similar manner, we have diffusive heat transport [20] in the outer segment for hybrid and full thermal equilibration, leading to a length dependent CCC. For all the choices of $\{\nu, \nu_i\}$, we find

$$\begin{aligned} F_1 = F_2 &\approx 0.13 + 0.26\sqrt{L_A/l_{\text{eq}}^{\text{th}}}, \\ F_c &\approx 0.07 - 0.26\sqrt{L_A/l_{\text{eq}}^{\text{th}}}. \end{aligned} \quad (21)$$

III. THE NOISY $5e^2/9h$ QPC PLATEAU

Here, we show how the $5e^2/9h$ QPC conductance plateau can appear only in the unequilibrated regime and compute shot noise at this plateau. We consider only the stochastic scenario. We note that if we consider the equilibration then it becomes exactly the same scenario of Section II.

The bare edge structure contains the counter-propagating $e/3$ (“innermost”), $e, e/3$ and $e/3$ (“outermost”) charge modes as we go from the bulk towards the edge; this is the reconstructed MacDonald edge [19]

(Fig. 4). We label the $e/3, e, e/3, e/3$ charge modes (from bulk to edge in the contacts) as “2”, “1”, “3”, “4”, respectively. At the QPC, we consider the case when the outermost $e/3$ mode is fully transmitted, the innermost $e/3$ mode is fully backscattered, and the remaining e and $e/3$ modes are renormalized to the KFP RG fixed point [4], giving rise to counter-propagating $2e/3$ charge mode and a n_3 neutral mode. This regime will be called the KFP region. Similarly, we will call the WMG regime the case where the renormalized (at the WMG RG fixed point [19]) charge modes $e/3, e/3$ counter-propagate to the n_1, n_2 neutral modes between each contact and the QPC.

Following Section II A, let us then assume that the renormalized modes emerge from the contacts (Fig. 4), and that we have incoherent scattering of wavepackets in each region of size l'_{RG} near the QPC. These processes are quantified by the density kernel matrices S_1, S_1', S_1'', S_1''' [25]. We point out that S_1' and S_1''' are responsible for stochastic processes where incoming charge is split between the outgoing modes, while S_1 and S_1'' bear the deterministic processes, where incoming charge has only a single outgoing mode to proceed to. Explicitly, we write

$$\begin{aligned} S_1 &= \begin{pmatrix} T_{11} & R_{21} & R_{31} \\ R_{12} & T_{22} & R_{32} \\ R_{13} & R_{23} & T_{33} \end{pmatrix} = S_1'', \\ S_1' &= \begin{pmatrix} \langle T'_{11} \rangle & \langle R'_{21} \rangle & \langle R'_{31} \rangle \\ \langle R'_{12} \rangle & \langle T'_{22} \rangle & \langle R'_{32} \rangle \\ \langle R'_{13} \rangle & \langle R'_{23} \rangle & \langle T'_{33} \rangle \end{pmatrix} = S_1'''. \end{aligned} \quad (22)$$

We note that the outermost $e/3$ mode does not take part in the noise generation but does enter the calculation of the transmission coefficient. In a similar manner as before, we write

$$\langle Q_1 \rangle = \frac{e}{3} \left[\frac{T_{11} \langle T'_{11} \rangle}{1 - \langle R'_{12} \rangle R'_{21} \langle R'_{12} \rangle R_{21}} \right]. \quad (23)$$

We use $T_{11} = 1, \langle T'_{11} \rangle = 1/2, \langle R'_{12} \rangle = \langle R'_{12} \rangle = 1/2, R'_{21} = R_{21} = 1$ to find $\langle Q_1 \rangle = 2e/9$ and $\langle Q_2 \rangle = e/9$. The source current is $I = 2e/3\tau$ and the transmission coefficient is then $t = (\langle Q_1 \rangle + e/3)/\tau I = 5/6$ and the QPC conductance plateau is at $G_{D_1} = 5/9$.

The current autocorrelation at D_1 is $\delta^2 Q_1 = \langle Q_1^2 \rangle - \langle Q_1 \rangle^2 = \langle Q_1 \rangle (e/3 - \langle Q_1 \rangle)$. Since $\langle Q_1^2 \rangle = e \langle Q_1 \rangle / 3$, we obtain $\delta^2 Q_1 = 2e^2/81$. Similarly, for the autocorrelation $\delta^2 Q_2 = \langle Q_2^2 \rangle - \langle Q_2 \rangle^2$ at D_2 we obtain $\delta^2 Q_2 = 2e^2/81$, while the crosscorrelation $\delta^2 Q_c = \langle Q_1 Q_2 \rangle - \langle Q_1 \rangle \langle Q_2 \rangle = -\langle Q_1 \rangle \langle Q_2 \rangle$ (since $\langle Q_1 Q_2 \rangle = 0$) becomes $\delta^2 Q_c = -2e^2/81$. The Fano factors are

$$F_i = \frac{\delta^2 Q_i}{e\tau I t(1-t)}, \quad i \in \{1, 2, c\}, \quad (24)$$

and therefore we find them to be $F_1 = F_2 = -F_c \approx 0.266$.

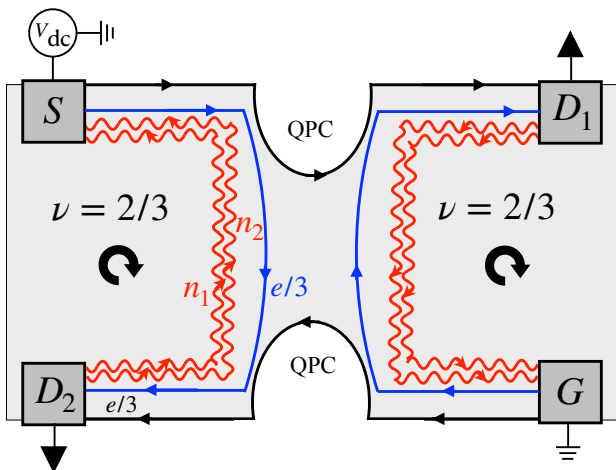


FIG. 5. The unequilibrated stochastic scenario for the $1/3$ QPC conductance plateau, where the renormalized modes emanate from the contacts. We refer to Fig. 2 for the geometry. Here the modes (going from the bulk towards the edge) are $n_1, n_2, e/3$ (inner), $e/3$ (outer). We denote by n_1, n_2 the neutral modes, which we draw as the wiggly red. At the QPC, the inner $e/3$ charge mode gets backscattered completely while the outer $e/3$ charge mode gets transmitted fully.

IV. THE NOISY $e^2/3h$ QPC PLATEAU

Here, we show how $e^2/3h$ QPC conductance plateau (experimentally discovered in Ref. 17, following earlier theoretical works in Refs. 39 and 40) can appear both in the unequilibrated (only the stochastic scenario) and equilibrated regimes. We compute the shot noise at this plateau and show that different inequalities hold among the autocorrelations and crosscorrelation for the different scenarios.

A. Unequilibrated scenario

We consider the renormalized (at the WMG RG fixed point [19]) reconstructed MacDonald edge structure, which consists of the $n_1, n_2, e/3$ (inner) and $e/3$ (outer) modes (from bulk to edge), where n_1, n_2 denote the neutral modes (Fig. 5). A plateau is observed at transmission $t = 1/2$, leading to $(G_{D_1} e^2)/h$ QPC conductance plateau, where $G_{D_1} = tI\tau/e$ and I is the source current, when the inner $e/3$ charge mode is fully backscattered and the outer $e/3$ charge mode is fully transmitted [17]. The neutral modes counter-propagate with respect to the charge modes and are fully backscattered at the QPC. We calculate the shot noise below following Refs. 39 and 40.

The source biases the two $e/3$ charge modes. We assume that N quasiparticles each having charge $e/3$ emanate from S into each charge mode in a time interval τ . Near the lower right side of QPC, upon equilibration $N_1 = N/2$ quasiparticles populate each mode and neutralons are created. These neutralons move to the upper

right side of QPC via the neutral modes and randomly decay into quasihole-quasiparticle pairs in the adjacent charge modes [40]. This decay process is stochastic and lead to N_1 and $(N - N_1)$ electronic excitations in the inner and outer modes, respectively, which reach D_1 and D_2 and generate nonzero dc shot noises but zero dc current. In a similar manner, near the upper left side of QPC equilibration takes place, and after equilibration $N_2 = N/2$ quasiparticles present in both modes. This process also creates neutral excitations which move to the lower left side of QPC and stochastically decay into $(N - N_2)$ and N_2 electronic excitations in the inner and outer modes, respectively, which reach D_2 and D_1 and generate shot noise.

We introduce random variables a, b , assuming the values ± 1 with equal probability, which characterize the neutral decay processes near upper right side and lower left side of QPC, respectively. We have $\langle a_m^{p/q} \rangle = \langle b_m^{p/q} \rangle = 0$. Here p stands for the inner $e/3$ charge mode and q stands for the outer $e/3$ charge mode. We note that a and b are mutually uncorrelated and use the following properties.

$$\begin{aligned} \langle a_m^p a_n^q \rangle &= \langle b_m^p b_n^q \rangle = \delta_{m,n} \delta_{p,q}, \\ \langle a_m^p a_n^q \rangle &= \langle b_m^p b_n^q \rangle = -\delta_{m,n} \text{ for } p \neq q. \end{aligned} \quad (25)$$

The charges Q_1 and Q_2 reaching at drains D_1 and D_2 during time τ are thus

$$\begin{aligned} Q_1 &= eN_1/3 + eN_1/3 + e/3 \sum_{i=1}^{N_1} a_i^p + e/3 \sum_{j=1}^{N_2} b_j^q, \\ Q_2 &= eN_2/3 + eN_2/3 + e/3 \sum_{k=1}^{N-N_1} a_k^q + e/3 \sum_{l=1}^{N-N_2} b_l^p. \end{aligned} \quad (26)$$

The total current is

$$I = \frac{\langle Q_1 \rangle + \langle Q_2 \rangle}{\tau} = \frac{2eN}{3\tau}, \quad (27)$$

the transmission through QPC is

$$t = \frac{\langle Q_1 \rangle}{\langle Q_1 \rangle + \langle Q_2 \rangle} = \frac{1}{2}, \quad (28)$$

and the QPC conductance plateau is at $G_{D_1} = 1/3$. The autocorrelation at D_1 is then

$$\begin{aligned} \delta^2 Q_1 &= \langle (Q_1 - \langle Q_1 \rangle)^2 \rangle \\ &= \frac{e^2}{9} \left\langle \left(\sum_{i=1}^{N_1} a_i^p + \sum_{j=1}^{N_2} b_j^q \right) \left(\sum_{m=1}^{N_1} a_m^p + \sum_{n=1}^{N_2} b_n^q \right) \right\rangle \\ &= \frac{e^2 N}{9}. \end{aligned} \quad (29)$$

Similarly we obtain for the autocorrelation at D_2 , $\delta^2 Q_2 =$

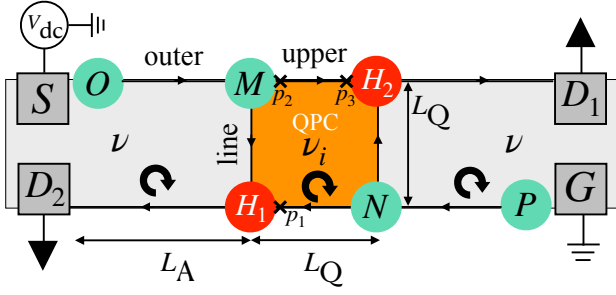


FIG. 6. The equilibration scenario for the $1/3$ QPC conductance plateau. The setup is similar to Fig. 3, but now we have $\nu > \nu_i$. Hot spots H_1, H_2 (red circles) occur due to the voltage drops and noise spots M, N, O, P (green circles) [20] result thereby.

$\langle(Q_2 - \langle Q_2 \rangle)^2\rangle = e^2 N/9$, whereas the crosscorrelation is

$$\begin{aligned} \delta^2 Q_c &= \langle(Q_1 - \langle Q_1 \rangle)(Q_2 - \langle Q_2 \rangle)\rangle \\ &= \frac{e^2}{9} \left\langle \left(\sum_{i=1}^{N_1} a_i^p + \sum_{j=1}^{N_2} b_j^q \right) \left(\sum_{k=1}^{(N-N_1)} a_k^q \right. \right. \\ &\quad \left. \left. + \sum_{l=1}^{(N-N_2)} b_l^p \right) \right\rangle \\ &= -\frac{e^2 N}{9}. \end{aligned} \quad (30)$$

Finally, the Fano factor for autocorrelation at D_1 is [39, 40]

$$F_1 = \frac{\delta^2 Q_1}{e\tau I t(1-t)} = 2/3, \quad (31)$$

and similarly we have $F_2 = -F_c = 2/3$.

B. Equilibrated scenario

We derive the general expressions for the CCC (shot noise) in a QPC for the bulk filling ν and QPC filling ν_i when $\nu > \nu_i$ (Fig. 6). We assume that the charge is fully equilibrated, hence charge transport is ballistic, moving downstream along each segment of the setup. We call the direction opposite to charge flow (upstream) antiballistic. Thereafter, we compute the values of CCC for specific choices of $\{\nu, \nu_i\}$ and for different thermal equilibration regimes. We assume that there is no bulk-leakage [32–35]. We study the scenarios employing two pictures for the thermal equilibration, which were introduced in Ref. 26 and Ref. 41, respectively. The experimental situation may be expected to be intermediate between these two pictures.

1. The picture of Ref. 26

Here the picture is that each of the modes creates noise by producing particle-hole pairs at the noise spots due to very short charge equilibration length. These processes lead to local heat equilibration by transferring heat energy among the modes. Thereby, all the modes acquire a common temperature, leading to CCC which is independent of length (c.f. Fig. 6).

We follow Refs. 20 and 36 and recompute the expressions of $\delta^2 I_1$ (autocorrelation in drain D_1), $\delta^2 I_2$ (autocorrelation in drain D_2) and $\delta^2 I_c$ (crosscorrelation) (Fig. 6) in the same spirit of Section II.

We write

$$\begin{aligned} \Delta I_1 &= \Delta I_u + \Delta I_r, \\ \Delta I_2 &= \Delta I_d + \Delta I_l, \\ \Delta I_S &= \Delta I_u + \Delta I_l, \\ \Delta I_G &= \Delta I_d + \Delta I_r, \end{aligned} \quad (32)$$

and

$$\begin{aligned} \Delta I_l &= (\nu - \nu_i) \frac{e^2}{h} \Delta V_M + \Delta I_l^{\text{th}}, \\ \Delta I_u &= \nu_i \frac{e^2}{h} \Delta V_M + \Delta I_u^{\text{th}}, \\ \Delta I_r &= (\nu - \nu_i) \frac{e^2}{h} \Delta V_N + \Delta I_r^{\text{th}}, \\ \Delta I_d &= \nu_i \frac{e^2}{h} \Delta V_N + \Delta I_d^{\text{th}}. \end{aligned} \quad (33)$$

Thereby, we find

$$\begin{aligned} \Delta I_1 &= \nu_i \frac{e^2}{h} \Delta V_M + \Delta I_u^{\text{th}} + (\nu - \nu_i) \frac{e^2}{h} \Delta V_N + \Delta I_r^{\text{th}} \\ &= \frac{\nu_i}{\nu} \Delta I_S + \frac{(\nu - \nu_i)}{\nu} \Delta I_G \\ &\quad + \frac{(\nu - \nu_i)}{\nu} (\Delta I_u^{\text{th}} - \Delta I_d^{\text{th}}) + \frac{\nu_i}{\nu} (\Delta I_r^{\text{th}} - \Delta I_l^{\text{th}}) \end{aligned} \quad (34)$$

and

$$\begin{aligned} \Delta I_2 &= \frac{\nu_i}{\nu} \Delta I_G + \frac{(\nu - \nu_i)}{\nu} \Delta I_S \\ &\quad + \frac{(\nu - \nu_i)}{\nu} (\Delta I_d^{\text{th}} - \Delta I_u^{\text{th}}) + \frac{\nu_i}{\nu} (\Delta I_l^{\text{th}} - \Delta I_r^{\text{th}}). \end{aligned} \quad (35)$$

Employing the local Johnson-Nyquist relations for thermal noise,

$$\begin{aligned} \langle(\Delta I_l^{\text{th}})^2\rangle &= \frac{2e^2}{h} (\nu - \nu_i) k_B T_M, \\ \langle(\Delta I_u^{\text{th}})^2\rangle &= \frac{2e^2}{h} \nu_i k_B T_M, \\ \langle(\Delta I_r^{\text{th}})^2\rangle &= \frac{2e^2}{h} (\nu - \nu_i) k_B T_N, \\ \langle(\Delta I_d^{\text{th}})^2\rangle &= \frac{2e^2}{h} \nu_i k_B T_N, \\ \langle(\Delta I_i^{\text{th}} \Delta I_j^{\text{th}})\rangle &= 0, \text{ for } i \neq j \text{ and } i, j \in \{l, u, r, d\}, \end{aligned} \quad (36)$$

we find the correlations to be

$$\begin{aligned} \delta^2 I_1 &= 2 \left(\frac{e^2}{h} \right) \frac{\nu_i}{\nu} (\nu - \nu_i) k_B (T_M + T_N) \\ &+ \frac{1}{\nu^2} \left[\nu_i^2 \langle (\Delta I_S)^2 \rangle + (\nu - \nu_i)^2 \langle (\Delta I_G)^2 \rangle \right], \end{aligned} \quad (37)$$

$$\begin{aligned} \delta^2 I_2 &= 2 \left(\frac{e^2}{h} \right) \frac{\nu_i}{\nu} (\nu - \nu_i) k_B (T_M + T_N) \\ &+ \frac{1}{\nu^2} \left[\nu_i^2 \langle (\Delta I_G)^2 \rangle + (\nu - \nu_i)^2 \langle (\Delta I_S)^2 \rangle \right], \end{aligned} \quad (38)$$

and

$$\begin{aligned} \delta^2 I_c &= -2 \left(\frac{e^2}{h} \right) \frac{\nu_i}{\nu} (\nu - \nu_i) k_B (T_M + T_N) \\ &+ \frac{\nu_i (\nu - \nu_i)}{\nu^2} \left[\langle (\Delta I_G)^2 \rangle + \langle (\Delta I_S)^2 \rangle \right], \end{aligned} \quad (39)$$

where T_M, T_N are, respectively, the temperatures at the noise spots M and N , which are found by solving self-consistent equilibration equations and considering energy conservation at each edge mode junction [20, 36]. We note that the dissipated powers at the hot spots take the form

$$P_{H_1} = P_{H_2} = \frac{e^2 V_{dc}^2 \nu_i (\nu - \nu_i)}{h 2\nu}. \quad (40)$$

The contributions $\langle (\Delta I_G)^2 \rangle = \langle (\Delta I_S)^2 \rangle$ at the noise spots O and P are computed by evaluating integrals, as shown in Ref. 20 and 36, assuming that no voltage drops take place along the outer segment and the lead contacts remain at zero temperature..

Here we consider $\{\nu, \nu_i\} = \{2/3, 1/3\}$, and $\{2/3(r), 1/3\}$. As charge is fully equilibrated in each segment of the QPC set up (Fig. 6), we have $I_1 = e^2 V_{dc} / (3h)$ for each of the $\{\nu, \nu_i\}$ choices here, leading to transmission $t = 1/2$ and $G_{D_1} = 1/3$ [20].

For no thermal equilibration (considered also in Ref. 23 for a single edge segment), we have only ballistic and antiballistic heat transports in any segment of the QPC set up, leading to a constant CCC. Similarly, by following our assumptions as before, only upstream modes will contribute at O, P . For $\{\nu, \nu_i\} = \{2/3, 1/3\}$ we find

$$\begin{aligned} T_M &= T_N = \frac{eV_{dc}}{\sqrt{5}\pi k_B}, \\ \langle (\Delta I_S)^2 \rangle &= \langle (\Delta I_G)^2 \rangle \approx 0.044 \frac{e^3 V_{dc}}{h}, \end{aligned} \quad (41)$$

leading to $F_1 = F_2 \approx 0.35, F_c \approx -0.22$. For $\{\nu, \nu_i\} = \{2/3(r), 1/3\}$ we find

$$\begin{aligned} T_M &= T_N = \frac{3eV_{dc}}{4\sqrt{6}\pi k_B}, \\ \langle (\Delta I_S)^2 \rangle &= \langle (\Delta I_G)^2 \rangle \approx 0.06 \frac{e^3 V_{dc}}{h}, \end{aligned} \quad (42)$$

leading to $F_1 = F_2 \approx 0.28, F_c \approx -0.1$. Similarly, for hybrid and full thermal equilibration, we have diffusive heat transport in the outer segment and ballistic and antiballistic heat transports in the line and the upper segments of the QPC set up, leading to length dependent CCC. For each choice of $\{\nu, \nu_i\}$, we find [20]

$$\begin{aligned} F_1 &= F_2 \approx 0.09 + 0.3 \sqrt{L_A / l_{eq}^{th}}, \\ F_c &\approx 0.09 - 0.3 \sqrt{L_A / l_{eq}^{th}}. \end{aligned} \quad (43)$$

2. The picture of Ref. 41

Here, not all the modes reach a common temperature at the noise spot. Rather, the mode(s) going around the QPC slowly give up heat to the modes going around the bulk regions (c.f. Fig. 6). We calculate the noise in the no thermal equilibration regime by following the assumption of Ref. 41. We consider a scenario as in Fig. 6. Ref. 41 assumed that none of the modes acquire a common temperature at the noise spot. In addition, the mode with filling ν_i slowly gives heat to the mode with filling ν while travelling.

We write the differential equation for heat transport along the AB segment as [20]

$$\partial_x \begin{pmatrix} T^2(x) \\ T_i^2(x) \end{pmatrix} = \frac{1}{l_{eq}^{th}} \begin{pmatrix} -1 & 1 \\ -1 & 1 \end{pmatrix} \begin{pmatrix} T^2(x) \\ T_i^2(x) \end{pmatrix} - \frac{2P}{\kappa} \delta(x - x_{hot}), \quad (44)$$

where x_{hot} is the hotspot location and P is the power dissipated there. T and T_i are the temperature profiles for filling ν and ν_i , respectively. We find the diffusive temperature profiles for the AB segment as

$$\begin{aligned} T^2(x) &= c_1 + c_2 x, \\ T_i^2(x) &= c_1 + c_2 (x + l_{eq}^{th}). \end{aligned} \quad (45)$$

In addition, T_i^2 jumps by $2P/\kappa$ upon crossing the hotspot location $x = L_Q$ when going from the segment NH_1 to H_1M . Now one needs to impose the appropriate boundary conditions, solve for the temperature profiles, and thereby find the temperature $T_i(x=0)$ at the noise spot M .

One boundary condition is $T(x=0) = 0$, which gives $c_1 = 0$. Now, we consider three points p_1, p_2, p_3 as in the figure. From the symmetry of the system, we conclude that $T_i^2(x=p_1) = T_i^2(x=p_3)$. Also we note that $T_i^2(x=p_2) = T_i^2(x=p_3)$, since only the mode with filling ν_i is travelling from M to H_2 . Hence, we write

$$\begin{aligned} T_i^2(x=p_2) &= T_i^2(x=p_1), \\ c_2 l_{eq}^{th} &= c_2 (L_Q + l_{eq}^{th}) - \frac{2P}{\kappa}, \\ c_2 &= \frac{2P}{\kappa L_Q}. \end{aligned} \quad (46)$$

Thus, we find $T_i(x=0) = \sqrt{2Pl_{\text{eq}}^{\text{th}}/\kappa L_Q}$, leading to shot noise $\sim \sqrt{l_{\text{eq}}^{\text{th}}/L_Q}$.

V. SUMMARY AND OUTLOOK

In this work we have considered the $\nu = 2/3$ FQH state in a QPC geometry. We have studied both the bare and reconstructed edge structures that are consistent with the bulk-boundary correspondence. For each of these, we have considered the steady state of the edge modes to be either unequilibrated or equilibrated. In the unequilibrated regime, two different paradigms of RG fixed points have been proposed earlier, namely KFP [4] and WMG [19]. Recent experiments [21–24] have established that the thermal equilibration length is an order of magnitude large than the charge equilibration length. These findings imply that different degrees of thermal equilibration are possible, along with full equilibration as far as charge is concerned. In this study we have found that there are three possible QPC-generated two-terminal conductance plateaus, $e^2/2h$, $5e^2/9h$, and $e^2/3h$; there are several distinct scenarios (discussed above) that lead to the first and last conductance values. Experimentally, the $e^2/2h$ plateau has been reported recently [27, 28] and the $e^2/3h$ plateau was discovered earlier [17]. We predict that if one finds the $e^2/3h$ plateau, then another possible plateau can exist at $5e^2/9h$ if the edge modes are in the unequilibrated regime. To figure out in which regime we are in, we can use *electrical shot noise*, namely autocorrelations and crosscorrelation, at these plateaus. We have identified that distinct mechanisms are responsible for the existence of shot noise in different scenarios, leading to

different inequalities between them. Thus, our comprehensive study provides a classification of the steady state of the edge modes based on shot noise. Our proposal can be extended to other filling fractions [42] and can be tested in the experiments with present day technology.

ACKNOWLEDGMENTS

We thank Christian Glattli, Udit Khanna, Michael J. Manfra, Alexander D. Mirlin, Jinhong Park, Christian Spånslätt, and Kun Yang for useful discussions. We thank Christian Glattli also for sharing his unpublished data. S.M. was supported by the Weizmann Institute of Science, Israel Deans fellowship through Feinberg Graduate School, as well as the Raymond Beverly Sackler Center for Computational Molecular and Material Science at Tel Aviv University. A.D. was supported by DFG MI 658/10-2 and DFG RO 2247/11-1. A.D. also thanks the Israel Planning and budgeting committee (PBC) and the Weizmann Institute of Science, the Dean of Faculty fellowship, and the Koshland Foundation for financial support. A.D. thanks IISER Tirupati start-up grant for support. Y.G. acknowledges support by the DFG Grant MI 658/10-2, by the German-Israeli Foundation Grant I-1505-303.10/2019, by the ISF grant, by the DFG Grant RO 2247/11-1, and by the Minerva Foundation. Y.G. is the incumbent of InfoSys Chair. M.G. has been supported by the Israel Science Foundation (ISF) and the Directorate for Defense Research and Development (DDR&D) Grant No. 3427/21, the ISF grant No. 1113/23, and the US-Israel Binational Science Foundation (BSF) Grant No. 2020072.

-
- [1] D. C. Tsui, H. L. Stormer, and A. C. Gossard, Two-dimensional magnetotransport in the extreme quantum limit, *Phys. Rev. Lett.* **48**, 1559 (1982).
 - [2] R. B. Laughlin, Anomalous quantum hall effect: An incompressible quantum fluid with fractionally charged excitations, *Phys. Rev. Lett.* **50**, 1395 (1983).
 - [3] A. H. MacDonald, Edge states in the fractional-quantum-hall-effect regime, *Phys. Rev. Lett.* **64**, 220 (1990).
 - [4] C. L. Kane, M. P. A. Fisher, and J. Polchinski, Randomness at the edge: Theory of quantum hall transport at filling $\nu=2/3$, *Phys. Rev. Lett.* **72**, 4129 (1994).
 - [5] X. G. Wen, Electrodynamical properties of gapless edge excitations in the fractional quantum hall states, *Phys. Rev. Lett.* **64**, 2206 (1990).
 - [6] M. D. Johnson and A. H. MacDonald, Composite edges in the $\nu=2/3$ fractional quantum hall effect, *Phys. Rev. Lett.* **67**, 2060 (1991).
 - [7] R. C. Ashoori, H. L. Stormer, L. N. Pfeiffer, K. W. Baldwin, and K. West, Edge magnetoplasmons in the time domain, *Phys. Rev. B* **45**, 3894 (1992).
 - [8] M. Reznikov, M. Heiblum, H. Shtrikman, and D. Mahalu, Temporal correlation of electrons: Suppression of shot noise in a ballistic quantum point contact, *Phys. Rev. Lett.* **75**, 3340 (1995).
 - [9] T. Martin and R. Landauer, Wave-packet approach to noise in multichannel mesoscopic systems, *Phys. Rev. B* **45**, 1742 (1992).
 - [10] T. Martin, Noise in mesoscopic physics, *arXiv:cond-mat/0501208* (2005).
 - [11] R. de Picciotto, M. Reznikov, M. Heiblum, V. Umansky, G. Bunin, and D. Mahalu, Direct observation of a fractional charge, *Nature* **389**, 162 (1997).
 - [12] L. Saminadayar, D. C. Glattli, Y. Jin, and B. Etienne, Observation of the $e/3$ fractionally charged Laughlin quasiparticle, *Phys. Rev. Lett.* **79**, 2526 (1997).
 - [13] R. de Picciotto, M. Reznikov, M. Heiblum, V. Umansky, G. Bunin, and D. Mahalu, Direct observation of a fractional charge, *Physica B: Condensed Matter* **249-251**, 395 (1998).
 - [14] M. Reznikov, R. de Picciotto, M. Heiblum, D. C. Glattli, A. Kumar, and L. Saminadayar, Quantum shot noise, *Superlattices and Microstructures* **23**, 901 (1998).
 - [15] N. Batra and D. E. Feldman, Different fractional charges from auto- and cross-correlation noise in quantum hall

- states without upstream modes, *Phys. Rev. Lett.* **132**, 226601 (2024).
- [16] A. M. Chang and J. E. Cunningham, Transport evidence for phase separation into spatial regions of different fractional quantum hall fluids near the boundary of a two-dimensional electron gas, *Phys. Rev. Lett.* **69**, 2114 (1992).
- [17] A. Bid, N. Ofek, M. Heiblum, V. Umansky, and D. Mahalu, Shot noise and charge at the $2/3$ composite fractional quantum hall state, *Phys. Rev. Lett.* **103**, 236802 (2009).
- [18] A. Bid, N. Ofek, H. Inoue, M. Heiblum, C. L. Kane, V. Umansky, and D. Mahalu, Observation of neutral modes in the fractional quantum hall regime, *Nature* **466**, 585 (2010).
- [19] J. Wang, Y. Meir, and Y. Gefen, Edge reconstruction in the $\nu=2/3$ fractional quantum hall state, *Phys. Rev. Lett.* **111**, 246803 (2013).
- [20] C. Spånslätt, J. Park, Y. Gefen, and A. D. Mirlin, Conductance plateaus and shot noise in fractional quantum hall point contacts, *Phys. Rev. B* **101**, 075308 (2020).
- [21] S. K. Srivastav, R. Kumar, C. Spånslätt, K. Watanabe, T. Taniguchi, A. D. Mirlin, Y. Gefen, and A. Das, Vanishing thermal equilibration for hole-conjugate fractional quantum hall states in graphene, *Phys. Rev. Lett.* **126**, 216803 (2021).
- [22] R. A. Melcer, B. Dutta, C. Spånslätt, J. Park, A. D. Mirlin, and V. Umansky, Absent thermal equilibration on fractional quantum hall edges over macroscopic scale, *Nature Communications* **13**, 376 (2022).
- [23] R. Kumar, S. K. Srivastav, C. Spånslätt, K. Watanabe, T. Taniguchi, Y. Gefen, A. D. Mirlin, and A. Das, Observation of ballistic upstream modes at fractional quantum hall edges of graphene, *Nature Communications* **13**, 213 (2022).
- [24] S. K. Srivastav, R. Kumar, C. Spånslätt, K. Watanabe, T. Taniguchi, A. D. Mirlin, Y. Gefen, and A. Das, Determination of topological edge quantum numbers of fractional quantum hall phases by thermal conductance measurements, *Nature Communications* **13**, 5185 (2022).
- [25] I. Safi and H. J. Schulz, Transport in an inhomogeneous interacting one-dimensional system, *Phys. Rev. B* **52**, R17040 (1995).
- [26] S. Manna, A. Das, Y. Gefen, and M. Goldstein, Diagnostics of anomalous conductance plateaus in abelian quantum hall regime, [arXiv:2307.05173](https://arxiv.org/abs/2307.05173) (2023).
- [27] J. Nakamura, S. Liang, G. C. Gardner, and M. J. Manfra, Half-integer conductance plateau at the $\nu = 2/3$ fractional quantum hall state in a quantum point contact, *Phys. Rev. Lett.* **130**, 076205 (2023).
- [28] M. H. Fauzi, K. Nakagawara, K. Hashimoto, N. Shibata, and Y. Hirayama, Synthesizing $2h/e^2$ resistance plateau at the first landau level confined in a quantum point contact, *Communications Physics* **6**, 365 (2023).
- [29] H.-H. Lai and K. Yang, Distinguishing particle-hole conjugated fractional quantum hall states using quantum-dot-mediated edge transport, *Phys. Rev. B* **87**, 125130 (2013).
- [30] Y. Wang, V. Ponomarenko, Z. Wan, K. W. West, K. W. Baldwin, L. N. Pfeiffer, Y. Lyanda-Geller, and L. P. Rokhinson, Transport in helical luttinger liquids in the fractional quantum hall regime, *Nature Communications* **12**, 5312 (2021).
- [31] V. Ponomarenko and Y. Lyanda-Geller, Unusual quasiparticles and tunneling conductance in quantum point contacts in $\nu = 2/3$ fractional quantum hall systems, [arXiv:2311.05142](https://arxiv.org/abs/2311.05142) (2023).
- [32] C. Spånslätt, J. Park, Y. Gefen, and A. D. Mirlin, Topological classification of shot noise on fractional quantum hall edges, *Phys. Rev. Lett.* **123**, 137701 (2019).
- [33] M. Banerjee, M. Heiblum, V. Umansky, D. E. Feldman, Y. Oreg, and A. Stern, Observation of half-integer thermal hall conductance, *Nature* **559**, 205 (2018).
- [34] A. Aharon-Steinberg, Y. Oreg, and A. Stern, Phenomenological theory of heat transport in the fractional quantum hall effect, *Phys. Rev. B* **99**, 041302(R) (2019).
- [35] J. Park, C. Spånslätt, Y. Gefen, and A. D. Mirlin, Noise on the non-abelian $\nu = 5/2$ fractional quantum hall edge, *Phys. Rev. Lett.* **125**, 157702 (2020).
- [36] S. Manna, A. Das, M. Goldstein, and Y. Gefen, Full classification of transport on an equilibrated $5/2$ edge via shot noise, *Phys. Rev. Lett.* **132**, 136502 (2024).
- [37] Y. Meir, Composite edge states in the $\nu=2/3$ fractional quantum hall regime, *Phys. Rev. Lett.* **72**, 2624 (1994).
- [38] U. Khanna, M. Goldstein, and Y. Gefen, Fractional edge reconstruction in integer quantum hall phases, *Phys. Rev. B* **103**, L121302 (2021).
- [39] R. Sabo, I. Gurman, A. Rosenblatt, F. Lafont, D. Banitt, J. Park, M. Heiblum, Y. Gefen, V. Umansky, and D. Mahalu, Edge reconstruction in fractional quantum hall states, *Nature Physics* **13**, 491 (2017).
- [40] J. Park, B. Rosenow, and Y. Gefen, Symmetry-related transport on a fractional quantum hall edge, *Phys. Rev. Res.* **3**, 023083 (2021).
- [41] J. Park, C. Spånslätt, and A. D. Mirlin, Fingerprints of anti-pfaffian topological order in quantum point contact transport, *Phys. Rev. Lett.* **132**, 256601 (2024).
- [42] S. Manna and A. Das, Experimentally motivated order of length scales affect shot noise, [arXiv:2307.08264](https://arxiv.org/abs/2307.08264) (2023).